



401 N. Lindbergh Blvd.
St. Louis, MO 63141
Tel.: 314.993.1700, #546
Toll Free: 800.424.2841, #546
Fax: 800.708.1364
Cell: 314.283.1983

Send via email to: jbode@aaortho.org and cyoung@aaortho.org

**AAO Foundation Final Report Form
(a/o 1/3/2018)**

In an attempt to make things a little easier for the reviewer who will read this report, please consider these two questions before this is sent for review:

- Is this an example of your very best work, in that it provides sufficient explanation and justification, and is something otherwise worthy of publication? (We do publish the Final Report on our website, so this does need to be complete and polished.)*
- Does this Final Report provide the level of detail, etc. that you would expect, if you were the reviewer?*

Please prepare a report that addresses the following:

Type of Award

Biomedical Research Award

Name(s) of Principal Investigator(s)

Andrew Jheon

Institution

University of California San Francisco (UCSF)

Title of Project

Molecular profiling of the active periodontal ligament during mouse orthodontic tooth movement

Period of AAOF Support (e.g. 07-01-18 to 06-30-19):

07-01-18 to 12-31-19

Amount of Funding

\$30,000

Summary/Abstract

Please see below.

Response to the following questions:

1. Were the original, specific aims of the proposal realized? Yes, the original specific aims were realized. However, we are still in the process of performing RNAscope *in situ* hybridization of our identified, differentially expressed genes of interest. Once this is complete, we will submit our manuscript for publication.
2. Were the results published? These results have yet to be published but we are currently working on the manuscript.
 - a. If so, cite reference/s for publication/s including titles, dates, author or co-authors, journal, issue and page numbers.
 - b. Was AAOF support acknowledged?
 - c. If not, are there plans to publish? If not, why not?
3. Have the results of this proposal been presented? I was planning to present this project at the 2020 AAO meeting in May.
 - a. If so, list titles, author or co-authors of these presentation/s, year and locations
 - b. Was AAOF support acknowledged?
 - c. If not, are there plans to do so? If not, why not?
4. To what extent have you used, or how do you intend to use, AAOF funding to further your career? These small grants and projects aid in my exposure to the orthodontic community. The goal at the end of the funding period is submission of a manuscript in a peer-reviewed journal. However, this is not always possible due to the limited scope of these small grants. Invariably, these small grants do lead to preliminary data that can be utilized to apply for larger R03 or R01 grants from the NIH. I hope to use these small grants again in the future to develop novel ideas, generate preliminary data, and publish articles in peer-reviewed journals.

Summary

Central hypothesis: I hypothesized that narrowed and widened periodontal ligament (PDL)-spaces during orthodontic tooth movement (OTM), which represent PDL undergoing compression and tension, respectively, are correlated with changes in gene expression profiles and specific molecular signatures.

Specific Aim: To globally profile gene expression at specific regions experiencing differential PDL deformation during OTM.

Introduction: Despite the fact that orthodontics is considered to be the oldest dental specialty, there is yet little understanding of the molecular mechanisms involved in OTM. The PDL is essential for tooth anchorage to alveolar bone and maintains 100–300 μm of functional space in humans. The PDL is also essential for OTM evidenced by the loss of tooth movement with tooth ankylosis. External forces applied to the tooth crown are transferred to the viscoelastic elements contained within the PDL and shifts in magnitude and duration of forces result in different rates of formation and resorption of alveolar bone and cementum in the bone-PDL-tooth complex. However, the molecular effects of external forces on the PDL and how the PDL transfers these forces to elicit OTM is unclear. Although a handful of candidate genes have been shown to be expressed in the PDL, global gene expression profiling of narrowed and widened PDL-spaces during active OTM using next generation sequencing has yet to be performed. The global identification of differentially expressed genes in the PDL during active OTM will pinpoint individual genes for potential, future gene targeting strategies, as well as to identify novel gene pathways and networks that are important in OTM.

Methods:

Induction of OTM: OTM was induced on maxillary left 1st and 2nd molars in 6-week old Fvb mice for 2 days using elastic spacers of known stiffness values (Hygenic™ Elastidam, Coltene). During insertion of elastic spacers, animals were anesthetized with xylazine/ketamine. The contralateral right maxillary teeth served as controls. Mice were sacrificed after 2 days and the heads collected and fixed in 4% paraformaldehyde.

MicroCT analysis: MicroCTs were imaged at the Small ANimal Tomographic Analysis (SANTA) facility located at the Seattle Children's Research Institute using a Skyscan 1076 Micro-Computed Tomograph. Scans were performed at an isotropic resolution of 17.21 μm using the following settings: 55kV, 179A, 0.5mm Aluminum filter, 460ms exposure, rotation step of 0.7°, 180° scan, and 3 frame averaging. All data were reconstructed using Nrecon (Version 1.6.9.4) with the same grayscale threshold. Reconstructions were converted to 3D volumes using Drishti v2.4.

Collection of PDL tissue: The same specimens images by microCT scans were used to isolate PDL tissue. For laser microdissection tissue capture, the specimens were demineralized in 0.5M EDTA for 2 weeks, dehydrated, and processed using an ASP300S processor (Leica Microsystems) and sections were transferred onto MembraneSlide 1.0 PEN glass slides (Zeiss), which facilitate the cutting and collection of laser microdissected tissue. Serial 10 μm sections were prepared using a Reichert-Jung 820II microtome. Specific widened PDL-space regions were collected using laser microdissection technology (PALM LMD, Zeiss) at the Laboratory of Cell Analysis Core at UCSF.

RNA isolation: Total RNA were extracted from formalin-fixed, paraffin-embedded PDL tissue using the Pinpoint™ Slide RNA Isolation System II (Zymo Research), which is specifically designed to isolate RNA from laser microdissected tissues.

RNAseq and data analysis: RNAseq experiments were performed at the UCSF SABRE Center Functional Genomics Core Facility for high throughput sequencing (<http://www.arrays.ucsf.edu>). Briefly, total RNA quality was assessed by spectrophotometer (NanoDrop, Thermo Fisher Scientific Inc.) and the Agilent 2100 Bioanalyzer (Agilent Technologies). RNA sequencing libraries were generated according to the manufacturer's protocol (TruSeq stranded mRNA sample prep kit, Illumina) and indexed libraries were sequenced on the Illumina HiSeq 2500. Data analysis required demultiplexing the results, trimming adapter sequences from the reads, and aligning unique reads to the mouse genome (mm10). Sequence alignment and splice junction estimation were performed using Bowtie2 (<http://bowtie-bio.sourceforge.net/bowtie2/index.shtml>) and TopHat (<http://tophat.cbcb.umd.edu/>), respectively. For differential expression testing, the genomic alignments were restricted to those mapping to an annotated transcriptome provided by Ensembl.

qPCR: qPCR was performed on select genes of interest using PrimeTime primers (Integrated DNA Technologies) specific for *Tnc*, *Postn*, *Dkk3*, *Inhba*, *Gli2*, and *Sema3a*. qPCR reactions used the GoTaq qPCR Master Mix (Promega, San Luis Obispo, CA, USA) in a Mastercycler Realplex (Eppendorf, Hamburg, Germany), and conditions were: 95°C, 2 min; 40 cycles at 95°C, 15 s; 58°C, 15 s; 68°C, 20 s; followed by a melting curve gradient. Expression levels of the genes of interest were normalized to levels of *Rpl19* (Ribosomal protein L19).

Results: OTM was prompted for 2 days in 6-week old mice as shown (Fig. 1). We utilized a split mouth design so that OTM was induced on the 1st and 2nd molars in the left maxilla whereas the contralateral or right side was used as control (No OTM). Mouse heads were collected and microCT scans were performed. By using the split mouth experimental design, we could then overlay microCT scans from the right (control, No OTM) and left (OTM) maxilla to perform 3D site registration to quantify the amount of OTM (Fig. 2), if desired, as well as to isolate similar volumes of active PDL from control and OTM 1st molars. *In silico* transverse sections of microCT images were performed through the roots of the molars (Fig. 3). The distobuccal (DB) root of the 1st molar was chosen for PDL tissue collection and RNA isolation because this root appeared to be highly affected during OTM, evidenced by widened PDL space compared to the DB root of the contralateral 1st molar. Notably, the mesial root of the 2nd molar showed similarly widened PDL space and we could have easily opted to isolate this tissue rather than the 1st molar. The PDL space of the 1st molar DB root was analyzed from 3 male and 3 female mice and the average PDL space was documented (Fig. 4). One can observe the increased variability and range of PDL space undergoing OTM vs control. Male and female mice showed little difference.

We identified the largest PDL space in the DB root of the 1st molar from the microCT images (Fig. 5). To isolate PDL tissue and subsequently isolate RNA for RNAseq experiments, we serially sectioned the same samples that were scanned by microCT (Fig. 6). We identified the region of interest (widened PDL space) that we wanted to isolate based on the microCT images, and we essentially counted the number of slides to target the region of interest. We collected PDL tissue over 200-300um of the DB root length to isolate adequate total RNA for RNAseq experiments. To note, we also planned to isolate PDL tissue from narrowed PDL space but the high external forces utilized precluded our

ability to achieve this. In the future, we will have to decrease the external forces to allow for enough narrowed PDL tissue and RNA to be collected.

RNAseq analysis identified 88 differentially expressed (DE) genes between control and OTM PDL collected from the DB root of the 1st molar once we applied a false discovery rate (FDR) < 0.05. Applying a p-value < 0.01, 364 DE genes were identified (Fig. 7). Gene ontology (GO) analysis identified some interesting cellular pathways that may be affected, however, the significance of GO analysis may be questionable (Table 1). Thus, we proceeded to confirm the differential expression of several identified genes by qPCR (Fig. 8). Out of 6 DE genes tested, we confirmed that 5 of these genes, namely *Tnc*, *Postn*, *Gli2*, and *Sema3a* indeed showed differences in expression between control and OTM PDL. *Dkk3* and *Inhba* were not confirmed to be differentially regulated.

Final summary and future research plans: We have utilized 3D microCT imaging and analysis techniques to pinpoint the most widened PDL space in the DB root of the 1st molar during OTM. We then sectioned the same samples and identified the histological sections of interest for tissue laser microdissection of the widened PDL. We isolated 200-300um of PDL tissue and performed RNAseq. We identified numerous DE genes between control and OTM samples and thus far, we have confirmed differential expression of 5 genes using qPCR. We are currently performing *in situ* hybridization using RNAscope techniques to determine the spatial distribution of our identified DE genes. RNAscope experiments will also allow us to reconfirm RNAseq and qPCR data. I would like to confirm additional DE genes of interest and once the RNAscope experiments are completed, I will submit our manuscript for publication in a peer-reviewed journal.

In the future, I would like to acquire genetically modified mice inactivated for the confirmed DE genes of interest to perform OTM studies. Such studies will conclusively answer whether our identified DE genes of interest indeed play a role in OTM. In addition, we will further our mechanistic understanding of OTM at the cellular and molecular levels to ultimately, accelerate/reduce OTM, as well as to determine the precise external forces that should be applied for optimal OTM and reduced treatment times. Lastly, the data generated from our current study will be presented in an R03 proposal to the NIH to further continue our study of cellular and molecular responses by the PDL to varying external forces.

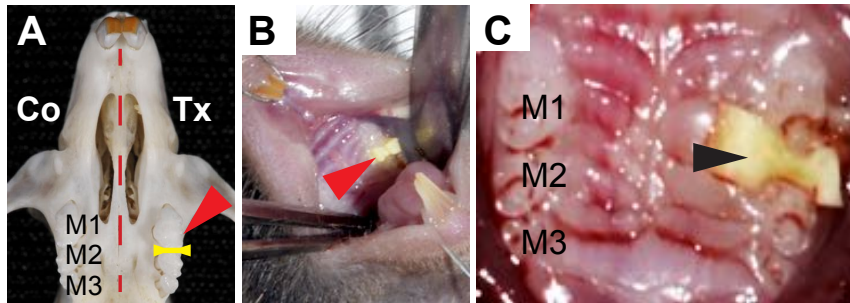


Figure 1. Experimental setup. (A) Maxilla of a mouse containing the 1st, 2nd, and 3rd molars (M1, M2, M3) illustrating the split mouth design with control (No OTM; right side) and OTM (left side) in the same mouse. The yellow line is a schematic representation of an elastic dam in between molars as indicated by a red arrowhead. (B,C) Images of elastic dams in between two molars in a mouse (arrowheads).

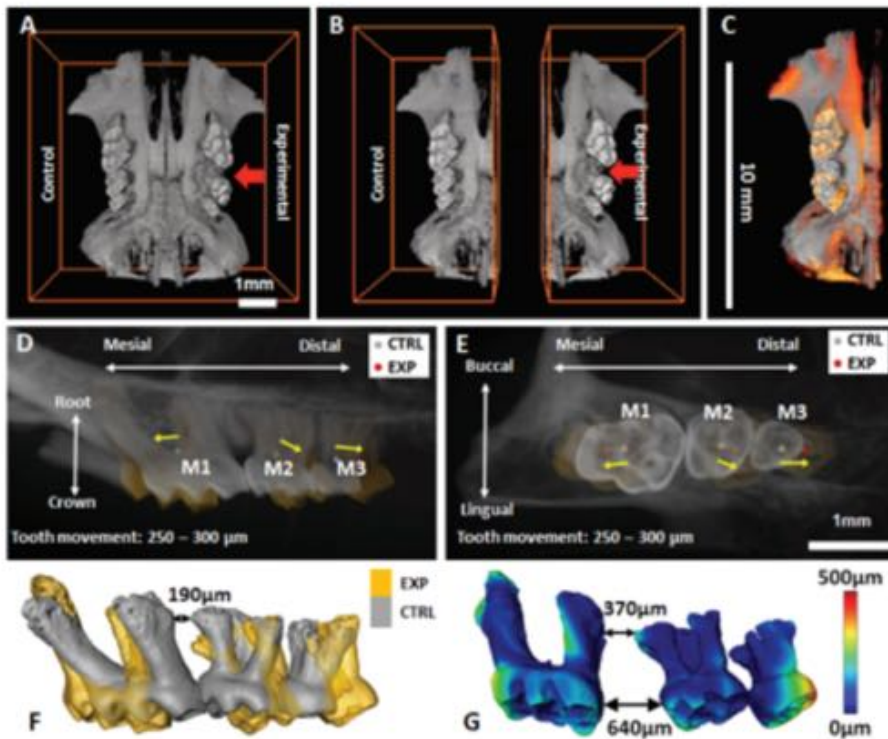


Figure 2. Image registration in 3D space: Red arrow highlights the location of an elastic band between maxillary 1st (M1) and 2nd (M2) molars. (A). Reconstructed volumes of control and experimental sides were digitally separated, and image registration was performed to illustrate gross movement of teeth relative to the whole hemi-maxillae (C) and for comparison. (D-G) The directions of respective movements of teeth are illustrated by a yellow vector from grey to red dots at the centers of rotation of respective molars. Tooth displacement of all the 3 molars (F) is mapped in the form of a color gradient (G) on the surface of the three molars (M1-M3).

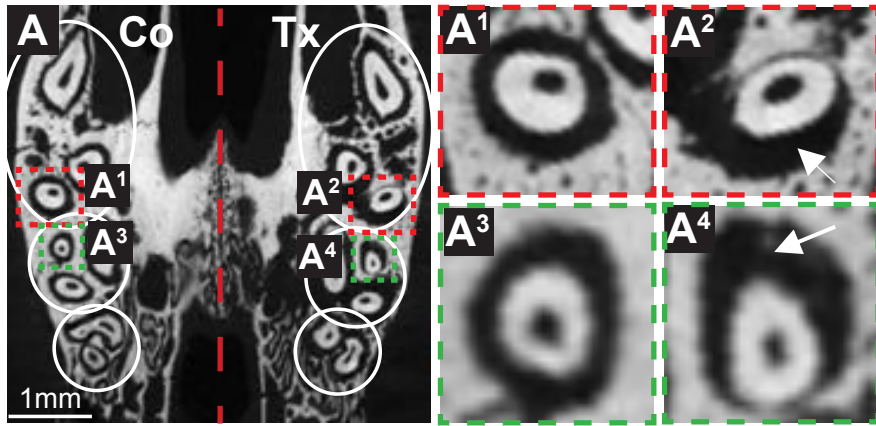


Figure 3. Cross-section of the roots of maxillary molars in . (A) *In silico* slice of a microCT through the midpoint of the roots of maxillary molars. The left side of the image represents the right side of the maxilla (Control, No OTM). The right side of the image represents the upper left maxilla where the 1st and 2nd molars are undergoing OTM. (A1, A2) Distobuccal root of the 1st molar on the control (A1) and OTM (A2) side. (A3, A4) Mesiobuccal root of the 2nd molar on the control (A3) OTM (A4) side. Note the widened PDL spaces undergoing tension (white arrows).

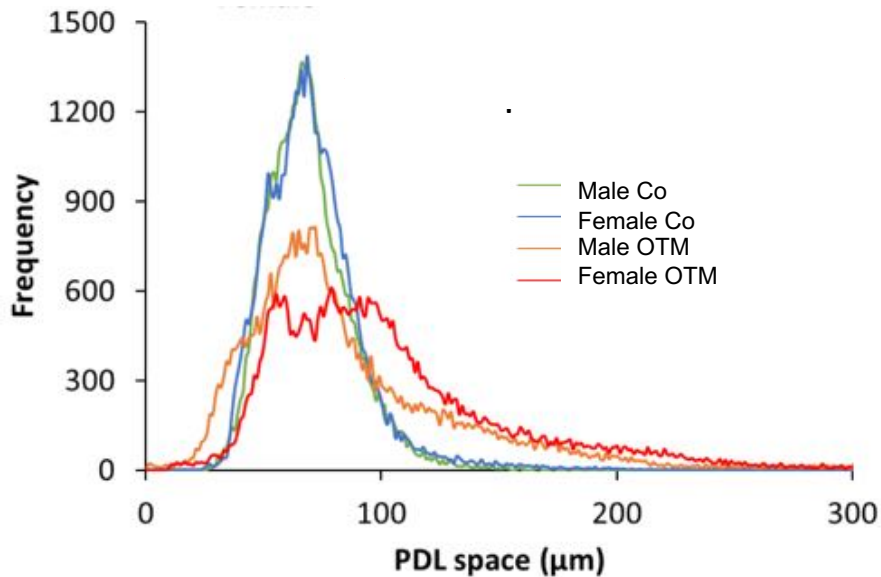


Figure 4. Map of the average changes in the PDL-space of the distobuccal root of M1 in male and female mice undergoing OTM. The M1s of 3 male and 3 female mice were analyzed for PDL-spaces. On the control side (No OTM), PDL-space showed a small range (~30-100μm), as expected, with a mean PDL-space of ~70μm. With OTM, the range of PDL-space increased dramatically (~20-200μm) reflecting the different PDL-spaces generated from OTM. The rubber dam was inserted between M1 and M2 for 2 days, and mouse heads were scanned using microCT.

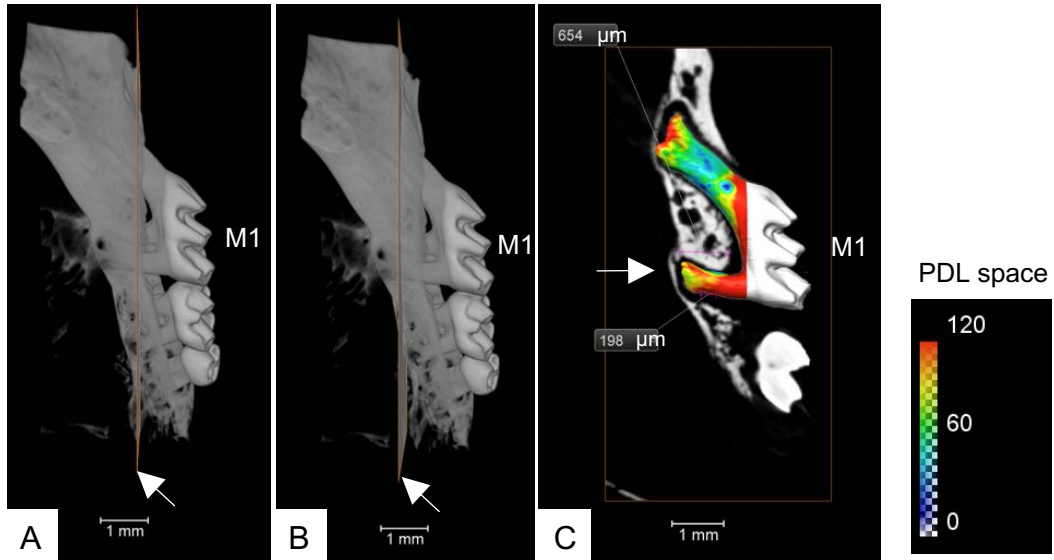


Figure 5. Representative microCT analysis of region of interest of the 1st molar (M1) undergoing OTM. (A,B) Based on the heatmap of PDL space in (C), the region of interest in the root of the distobuccal cusp of M1 was narrowed down to the PDL tissue lying between the lines indicated (arrows). (C) Heatmap highlighting the differences in PDL space in the distobuccal root of M1. The dominant widened and narrowed PDL-space were determined based on the normalized frequency vs. PDL space from control (No OTM) and experimental (OTM) groups. Only the OTM side is shown here. In this example, 24 slides of 10 μ m serial sections were selected for laser microdissection to capture tissue from widened PDL spaces. Similar volumes of PDL space were captured from M1 of the control side.

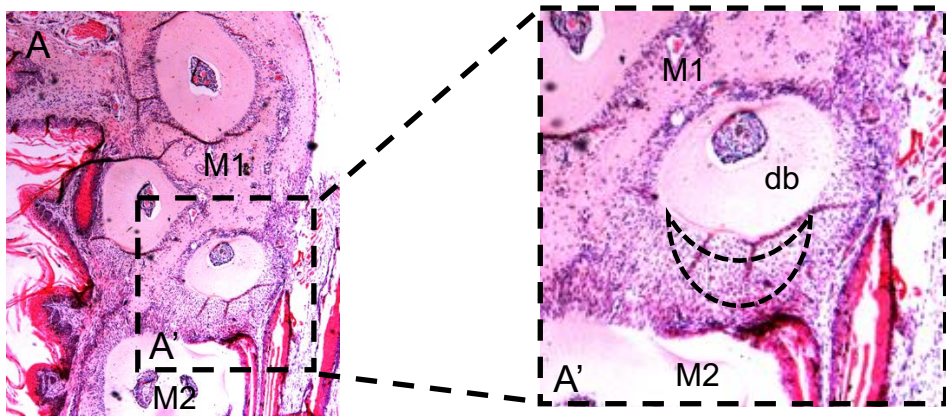


Figure 6. Histological section through the molar roots on the OTM side. (A) Hematoxylin and eosin staining of through the roots of M1 and M2 are shown in ventral view. (A') Magnified view of the distobuccal root showing the widened PDL-spaces undergoing tension. Crescent-shaped dotted line indicates the approximate location of laser microdissection. Approximately, 200-300 μ m of PDL tissue was collected from control (No OTM) and OTM M1 roots and total RNA was isolated for subsequent RNAseq and qPCR experiments.

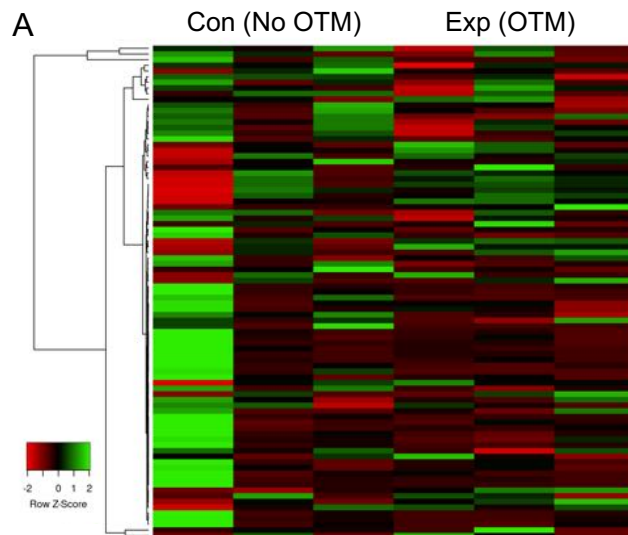


Figure 7. RNAseq data analysis. (A) Heatmap of 88 DE genes that showed 2-fold difference between control and OTM with an FDR<0.05. DE, differentially expressed; FDR, false discovery rate.

	Mus musculus (REF)		upload_1 (▼ Hierarchy NEW! ⓘ)				
GO cellular component complete	#	#	expected	Fold Enrichment	+/-	raw P-value	FDR
epidermal lamellar body	4	3	.06	47.04	+	1.28E-04	1.81E-02
↳lamellar body	16	5	.26	19.60	+	1.53E-05	2.76E-03
↳secretory granule	386	29	6.15	4.71	+	2.23E-11	2.21E-08
↳cellular anatomical entity	18638	327	297.17	1.10	+	5.58E-06	1.38E-03
↳secretory vesicle	596	31	9.50	3.26	+	2.06E-08	1.02E-05
↳vesicle	2039	55	32.51	1.69	+	1.39E-04	1.83E-02
connexin complex	20	5	.32	15.68	+	3.80E-05	5.79E-03
↳plasma membrane	5326	122	84.92	1.44	+	1.09E-05	2.15E-03
↳cell periphery	5473	127	87.26	1.46	+	3.00E-06	9.91E-04
↳gap junction	33	5	.53	9.50	+	3.04E-04	3.54E-02
cornified envelope	29	6	.46	12.98	+	1.58E-05	2.61E-03
keratin filament	42	7	.67	10.45	+	1.08E-05	2.37E-03
↳intermediate filament	129	12	2.06	5.83	+	2.41E-06	9.55E-04
↳intermediate filament cytoskeleton	165	13	2.63	4.94	+	5.07E-06	1.44E-03
extracellular space	1951	69	31.11	2.22	+	7.10E-10	4.69E-07
↳extracellular region	2797	94	44.60	2.11	+	3.02E-12	5.98E-09
cell surface	1165	35	18.58	1.88	+	4.49E-04	4.68E-02
nucleus	6824	77	108.80	.71	-	2.40E-04	2.98E-02
catalytic complex	1341	7	21.38	.33	-	4.16E-04	4.58E-02

Table 1. Gene ontology analysis. Potential cellular mechanisms affected in PDL undergoing tension was identified through between control and OTM with an FDR<0.05. DE, differentially expressed; FDR, false discovery rate.

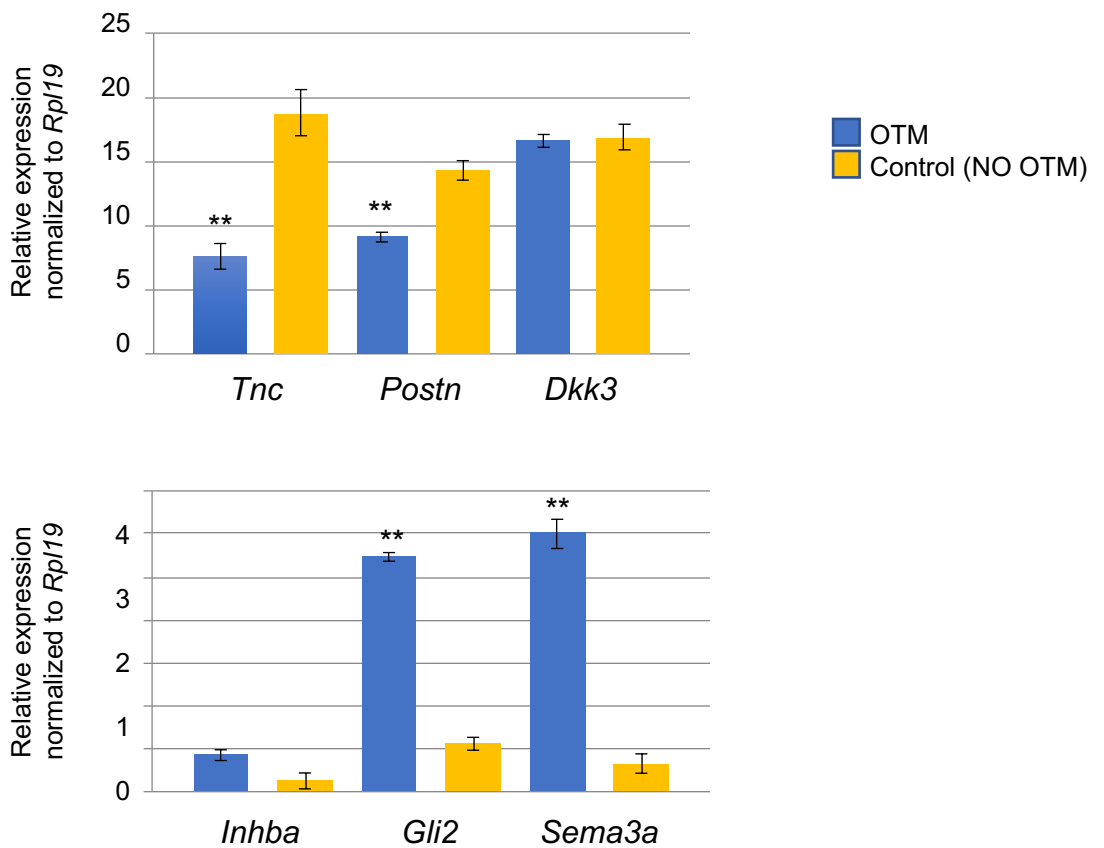


Figure 8. Confirmation of differentially expressed genes in the widened PDL space in mice undergoing no OTM (control) and OTM. *Tnc* and *Postn* were confirmed to be down-regulated in widened PDL during OTM. *Gli2* and *Sema3a* were confirmed to be up-regulated in widened PDL during OTM. *Rpl19* was assayed as the housekeeping gene.